Journal of Ultrafine Grained and Nanostructured Materials
https://jufgnsm.ut.ac.ir
Vol. 51, No.2, December 2018, pp. 153-162
Print ISSN: 2423-6845 Online ISSN: 2423-6837
DOI: 10.22059/JUFGNSM.2018.02.07

Mechano-chemical activation of MoO_3-CuO/C powder mixture to synthesis nano crystalline Mo-Cu alloy

Morteza Saghafi Yazdi*, Mohammad Talafi Noghani, Alireza Najari

Department of Materials Science and Engineering, Faculty of Engineering, Imam Khomeini International University.

Recieved: 20 April 2018; Accepted: 13 August 2018

** Corresponding author email: msaghafi@eng.ikiu.ac.ir*

ABSTRACT

In this study, a high energy planetary ball milling technique was used to synthesize nano-crystalline Mo-Cu alloys. Molybdenum trioxide (MoO_3) and copper oxide (CuO) were used as the starting materials. Carbo-thermal co-reduction of mixed Mo and Cu oxides powders was done with milling followed by a heat treatment at a high temperature. Differential thermal analysis/thermogravimetric (DTA/TG) was used to determine the heat treatment temperature of activated powders. X-ray diffraction (XRD) analysis was used to investigate the phase structure during the milling and heat treatment. Field emission scanning electron microscopy (FESEM) has been employed to investigate the morphology of powder particles. It was found that the complete carbo-thermal reduction of the oxides mixture may not be possible by the mechanical milling at the ambient temperature and based on thermodynamic investigations, thermal activation was necessary to reduce a MoO_3-CuO mixture to a metallic structure. Some peaks at 400, 600 and 950 °C from DTG results of the mixture sample milled for 10 h were observed which were related to the $Cu_6Mo_5O_{18}$, MoO_2-Cu and Mo formation during carbo-thermal reduction of the MoO_3-CuO mixture, respectively. XRD results showed 10 h milled sample after reduction at 1000 °C contained nano-crystalline Mo-Cu alloys with a mean crystallite size of 42 nm for Mo and 37 nm for Cu calculated by the Scherrer equation.

Keywords: *Nano-crystalline; Mechanical milling; Mo-Cu alloy; Nano particles; Refractory.*

1. Introduction

Copper alloys are widely used in industrial applications due to their high thermal and electrical conductivity, heat resistance, ablation resistance and high strength. Cu-W alloys are extensively used for the sweat cooling and electronic devices packaging and also as an electrical contact alloy [1-5]. Tungsten has a higher density, melting point and hardness than that of Mo that eliminates the application of Cu-W alloy. Molybdenum is a good candidate to be replaced with tungsten and sintering characteristics of Mo-Cu alloys are easier in comparison with W-Cu alloys. In a Mo-Cu system mixing produced heat is positive (+18 kJ/mole). There is a significant discrepancy in melting points and the lactic parameter of copper (T_{Cu} = 1083 °C, a_{Cu}= 0.361 nm) and molybdenum (T_{Mo} = 2625 °C, a_{Mo}= 0.314 nm) which the maximum solubility of molybdenum in the copper is 0.5 wt.% at 1100 °C [6, 7]. On the other hand Mo-Cu alloys are immiscible in liquid and solid states which means no alloy could be made using conventional equilibrium methods such as casting or liquid metallurgy [8]. In order to extend the solid solubility more than normal values some non-equilibrium processes such as rapid solidification, laser enhanced, vapor, ion beam or sputtering deposition, and mechanical alloying (MA) of elements could be used. Among

mentioned methods, MA is a simple method due to its ability to increase the solid solubility at the ambient temperature and this process could achieve a larger solid solubility extension. Plastic deformation of powder particles during MA caused a microstructure refinement of particles and increased the specific surface area. Stacking faults, vacancies and dislocation increased in the particles grains during the process of milling of the powder. Another advantage of mechanical milling is increasing the solid solubility of elements during the milling which could decrease the diffusion pathway in the mixture [9-12].

Many researches have been focused on the synthesis of Mo-Cu alloys with MA processes which resulted fine grain alloys with homogeneous microstructures and excellent properties [3, 10, 13-17]. In the fabrication of Mo-Cu alloys with the MA process, starting materials are usually mixed together into an element form in the ball milling system [14, 17, 18]. Sun et. al [8] synthesized novel core shell Cu-Mo nanoparticles via a simple ball-milling of a MoO_3-CuO mixture and a subsequent hydrogen reduction process. In some other works Mo-Cu were fabricated with combustion reactions using Al as a reducing agent [19]. Magnesio-thermal reduction of MoO_3-CuO mixture oxides was reported to be a high caloric process proceeded in combustion mode [7]. In the case of using reducing metals such as Al, Mg, Na or Ca, that is most of the time a challenging task to purify nano-crystalline powders from undesired byproducts. The advantage of using graphite as a reducing agent was that the CO_2 gas was a byproduct removed simultaneously during the reaction. Former studies have shown the formation of nano-crystalline metallic powders via the mechano-chemical reduction of NiO [20], V_2O_5 [21], CuO [22] and MoO_3 [23] with carbon and the effect of the milling processing on the metal oxides reduction was also reported. In this paper, a high energy planetary ball milling technique was used to synthesis nano-crystalline Mo-Cu alloy and mixed MoO_3-CuO was used as a starting material and graphite was used as the reducing agent.

2. Experimental procedure

Commercially pure MoO_3 (99.5%, 1-15 μm), CuO (99.9%, 0.5-2 μm) and carbon (99.2%, 0.5-5 μm) powders were weighed based on the reaction (1) and 40% mole extra carbon contents was used in this research. The excess carbon amount was used to provide the maximum contact area between the metal oxides/carbon particles. In the meantime, carbon may act as a diluent or lubricant during the milling process.

Another reason of using the excess carbon was the production of a CO/CO_2 mixture during the heat treatment of mixed powders. The calculation in this paper was based on the reaction 1 with the CO_2 production.

$$MoO_3 + CuO + 2C = Mo\text{-}Cu + 2CO_2 \quad (1)$$

Starting mixture materials were milled in the planetary ball mill (Sanat Ceram M.A) at the room temperature with the rotation speed of 120 rpm while the weight ratio of the ball (ball diameter: 11mm, hardness: 68HRC) to powder was fixed to be 20:1 in milled samples. A tube quartz furnace (Azar Furnace TFS/25-1250) under the argon protection was used to reduce activated samples at various temperatures for 1 h in the argon atmosphere. Bruker XRD instrument with Cu-K_α (λ=1.5405 Å, step size=0.04 degree) was employed for phase analysis of the prepared samples. The size of milled synthesized nano-crystallite powders and the crystallite size of annealed powders were measured by Williamson-Hall (eq. 1) and Sherrer (eq. 2) formulas respectively[24].

$$D = (0.9\lambda/\beta\cos\theta) + \eta\tan\theta \quad \text{(eq. 1)}$$

$$D = (0.9\lambda/\beta\cos\theta) \quad \text{(eq. 2)}$$

Where D is the mean crystallite size, λ is the X-ray wavelength, β is the line width at the one-half of the maximum intensity, η is the internal strain and θ is the Bragg angle (in degrees). A Linseis DTA/TG instrument was applied to determine the temperature of the heat treatment of the 10 h milled mixture in the nitrogen atmosphere as a protective environment and the heating rate was fixed to be 5 °C/min with Al_2O_3 as a crucible. FE-SEM (TESCAN MIRA3) was also used to investigate the morphology and particle size of the samples. The synthesized molybdenum-copper alloy were compressed in a pressure of 700 MPa (to prepare a disk with 9 mm diameter) in the hardened die and after that the sintering was done in the quartz tube of the furnace under the argon protection at 1050, 1100 and 1200 °C for 60 min as the stay time. Vickers hardness was used to measure the hardness of the sintered specimens (Koopa model: UV1, 10 kg).

Two wire method was used to measure the electrical conductivity (SIGMOR100 conductivity meter) of sintered materials. For measuring the hardness and electrical conductivity At least five tests were performed in each measurement to measure the hardness and electrical conductivity.

3. Results and discussion

Fig. 1 shows the XRD results of milled samples with milling times of 10 and 30 h. In both samples, peak broadening occurred and the intensities of MoO_3 and CuO peaks decreased because of the particles refinement and the residual strain in the powders. In fact metal oxides such as MoO_3 and CuO show brittle behaviors during the milling and their particles are fragmented continuously as the milling time gets extended in order to obtain particles in the nano scale. During the milling of the powder mixture, the compositional inhomogeneity decreased because of the severe plastic deformation, fracturing and re-welding of particles. Absence of graphite peaks in the milled samples for 10 h could be related to amorphous transformation of carbon atoms during the milling process. As shown in Figure 1 the graphite peak in the milled samples for 30 h was observed with a lower intensity as compared to an un-milled sample. In fact with extending the milling time from 10 to 30 h, the temperature on the contact area and the stored energy of the powder increases continuously and may cause to the recrystallization of the graphite powder at higher milling times.

The residual strain and crystallite size of MoO_3 and CuO in the sample milled for 30 h were calculated to be (1.7% and 22 nm) and (1.9% and 18 nm), respectively from the Williamson-Hall equation. In the literature it was shown that in the MoO_3-C mixture with increasing the milling time up to 200 h complete reduction couldn't be possible and MoO_3 was only reduced to MoO_2 during the solid state reduction [23]. The enthalpies and standard Gibbs free energy changes at 298 K for some reactions are also shown in the table 1 using data in the literature [25].

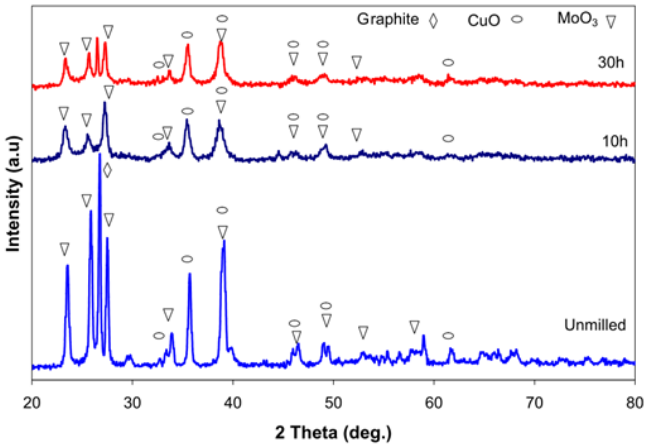

Fig. 1- XRD patterns of the samples milled for 10 and 30 h. The MoO_3 and CuO peaks tend to broaden and their intensities decrease during milling process.

Table 1- Thermodynamic parameters (enthalpies and standard Gibbs free energies) changes of the reduction reactions of Mo and Cu oxides by graphite [25]

Reaction	ΔG^0_{298} (kJ/mol.)	ΔH^0_{298} (kJ/mol.)	Reaction number
$MoO_3 + 0.5C = MoO_2 + 0.5CO_2$	-60.93	-39.4 0	(2)
$MoO_2 + C = Mo + CO_2$	+138.40	+194.90	(3)
$CuO + 0.25C = 0.5\ Cu_2O + 0.25CO_2$	-39.54	-23.00	(4)
$0.5Cu_2O + 0.25C = Cu + 0.25CO_2$	-23.11	-11.65	(5)
$Mo + 2C = Mo_2C$	-76.79	-52.3	(6)

Fig. 2 shows the relationship between the Gibbs free energy and the temperature for some reactions calculated theoretically using data in the literature [25]. The ΔG^0_{298} of the reactions (2), (4), (5) and (6) were negative and it was anticipated that these reactions could thermodynamically be accomplished during the milling at the room temperature. The carbo-thermal reduction of MoO_2 to molybdenum needed a higher temperature and reaction (3) showed above a 100 kJ/mol barrier to progress, although that was too high for the ball milling process to afford in the room temperature [21]. Therefore, the reduction reaction was actually stopped. Ball milling could be possibly overcome the thermodynamic barrier of 10-20 kJ/mol due to the structural defects formation in the powder during the milling [21]. The dependence of the standard Gibbs free energy on the temperature for the carbo-thermal reduction of mixed oxides based on reactions (1) was calculated theoretically and is shown in the equation 3:

$$\Delta G^0_T = 1.167 \times 10^{+5} - 217T + 0.059T^2 + 2.53 \times 10^{+5}\frac{1}{T} - 7.65 \times 10^{-6}T^3 - 25.24TlnT \qquad \text{(eq. 3)}$$

In fact the reaction (1) is the sum of reactions (2), (3), (4) and (5) that with eq. 3 the standard Gibbs free energy of reaction (1) could be measured directly at any temperature above the room temperature.

As shown in Fig. 2, the value of the barrier for all reactions decreased with the temperature increment, but it was revealed that for the reaction (3) the temperature required to be high enough to decrease the thermodynamic barrier. Thus, a higher temperature reduction was employed to produce Mo-Cu alloys from the MoO_3-CuO mixture with the mechanically activated carbon. In the case of the mechano-chemical reduction of MoO_3 and CuO with Al as the reducing agent, the standard Gibbs free energies for the reaction was reported -915 and -393 kJ/mole, respectively that indicated exothermic behaviour of the reaction and could be taken place during the milling with a high speed [25-27]. The reaction rate between MoO_3-CuO and carbon during the ball milling could be low because of the high thermodynamic barrier at the room temperature. The subsequent heat treatment was needed to complete the reduction and DTA/TG analyses were done to understand the details of the reduction process and the heat treatment temperature.

Fig. 3 shows FESEM images of the 10 h milled sample at different magnefications. As shown in this figure after 10 h milling of the MoO_3-CuO and carbon mixture the size of powders became very small and no extra milling times were needed. The carbon in the powder mixture was used as a reducing agent and also a lubricating material which caused to the formation of small

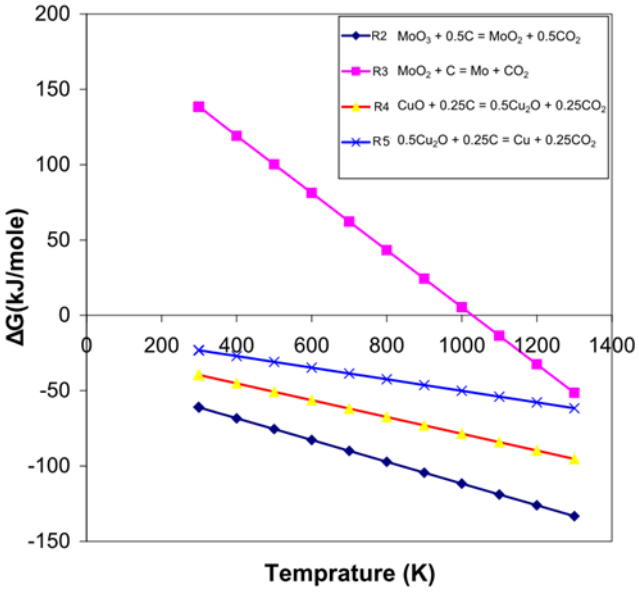

Fig. 2- Standard changes of free energy (ΔG°) of the reactions as a function of temperature. The magnitude of the thermodynamic barrier for all reactions becomes less at higher temperatures.

agglomerates of reduced paricles. As stated before with increasing the milling time from 10 to 30 h, the stored energy in the mixture also increased but during the heat treatment for synthesis of Mo-Cu at 1000 °C, the internal strain of nano powders would be released and the residual strain is not an important parameter to choose the 30 h milled sample for the heat treatment.

Fig. 4 shows the DTA/TG results of a 10 h milled mixture sample. To investigate the phase formation underlying every peak, this sample was reduced at high temperatures followed by an XRD investigation. Some peaks at 400, 600 and 950 °C from DTG results of the mixed sample milled for 10 h were observed during the carbothermal reduction of the MoO_3-CuO mixture. In the corresponding TG curve as is shown in this figure, weight losses are occurred in all peaks which show CO/CO_2 formation during the reduction. The total weight loss of the samples after the treatment was measured to be 35% which is in the good agreement with the theoretical value of 34.5%

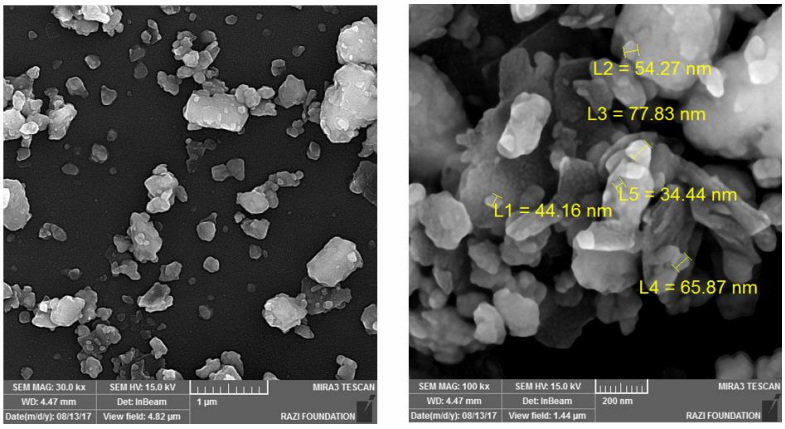

Fig. 3- FESEM images of 10 h milled sample at different magnefication. 10 h milling of MoO_3-CuO and carbon mixture is enough time to particles size of mixture becomes in nano-meter scale.

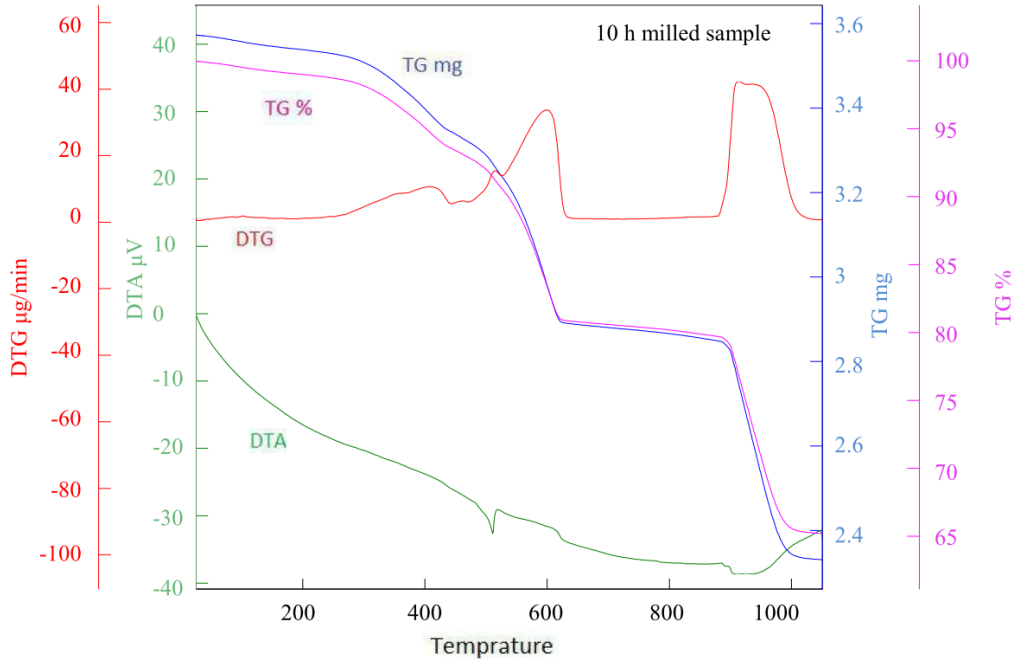

Fig. 4- DTA/TG traces of the sample milled for10 h. The DTA curve exhibited two endothermic peak at 520 and 950 °C, respectively which attributed to a stepwise carbothermic reduction of mixture oxide.

calculated from the reaction (1). The DTA curve exhibited two endothermic peaks at 520 and 950 °C, respectively attributed to a stepwise reduction of the mixture oxide.

Fig. 5 shows XRD results taken from the 10 h milled mixture reduced at different temperatures of 350, 450, 550 and 650 °C for 1h. The results show with annealing at 350 °C the $Cu_6Mo_5O_{18}$ complex phase was formed and with increasing the heat treatment temperature MoO_2 and Cu reflections started to appear. This figure shows $Cu_6Mo_5O_{18}$ peaks completely are disappeared when the temperature reached to 550 °C and the products were a mixture of MoO_2 and Cu. With increasing the reduction temperature from 550 to 650 °C the reduction of MoO_2 to Mo was not happened revealing that a higher temperature is needed for the progress of the reduction.

Fig. 5 also shows XRD patterns taken from the 10 h milled sample after the reduction at 800, 900 and 1000 °C. For the treated sample by heating at 800 °C, Mo, MoO_2 and Mo_2C peaks existed that with increasing the heat treatment temperature to 900 °C the intensity of MoO_2 and Mo_2C peaks decreased and the intensity of Mo peak intensity increased indicating the reaction of MoO_2 and

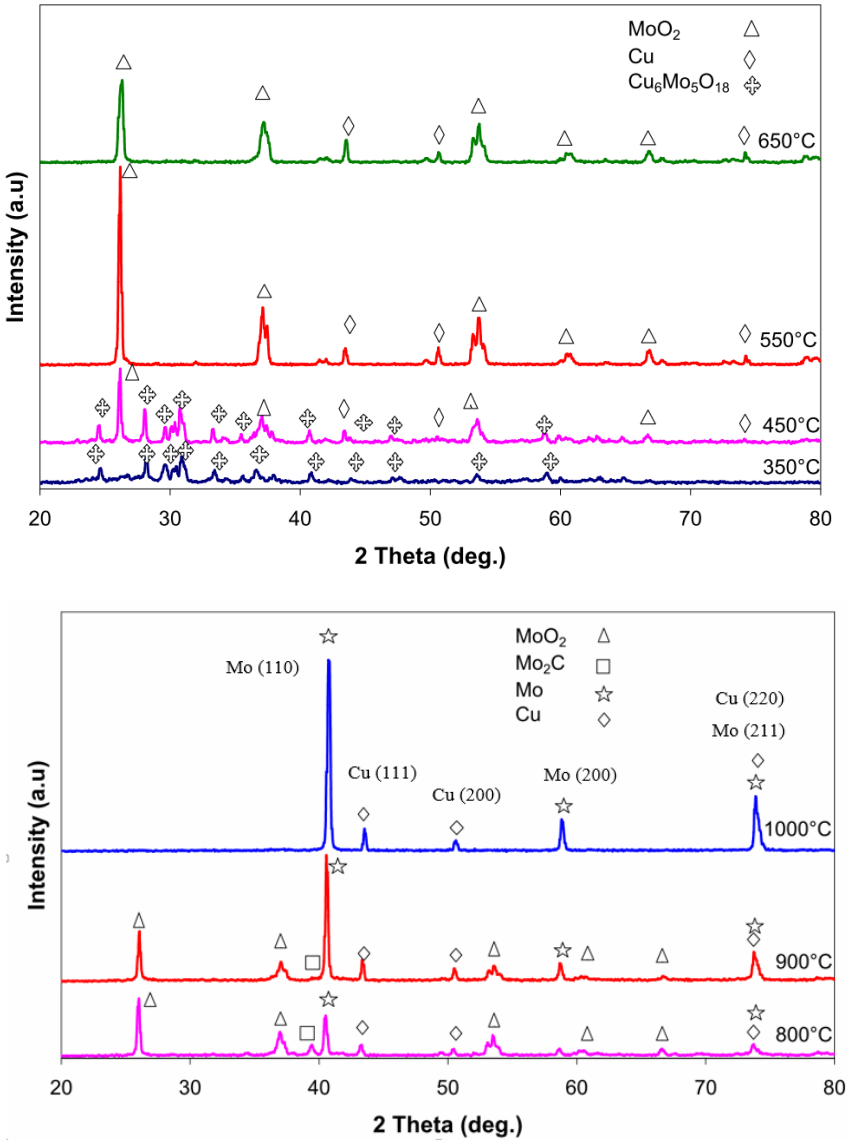

Fig. 5- (a) XRD patterns taken from the 10 h milled mixture after reduction at 350-1000 °C for 1 h. When the temperature reached to 1000 °C the only dominant phases are nano-crystalline Mo and Cu.

Mo_2C to produce Mo according to the reaction (7).

$$MoO_2 + 2Mo_2C = 5Mo + 2CO \quad (7)$$

In fact the peaks at 400, 600 and 950 °C from DTG results of the mixture sample milled for 10 h during the carbo-thermal procedure were related to the formation of $Cu_6Mo_5O_{18}$, MoO_2-Cu and Mo, respectively.

Eventually when the temperature reached 1000 °C the only dominant phases were nano-crystalline Mo and Cu that the intensities of the Cu(111), Cu(200), Cu(220), Mo(110), Mo(200), and Mo(211) peaks were observed. The reduction activity of the powders could enhance by the mechanical milling because of the increased contact areas of graphite and oxides as well as the stored energy in the particles. Presence of peaks

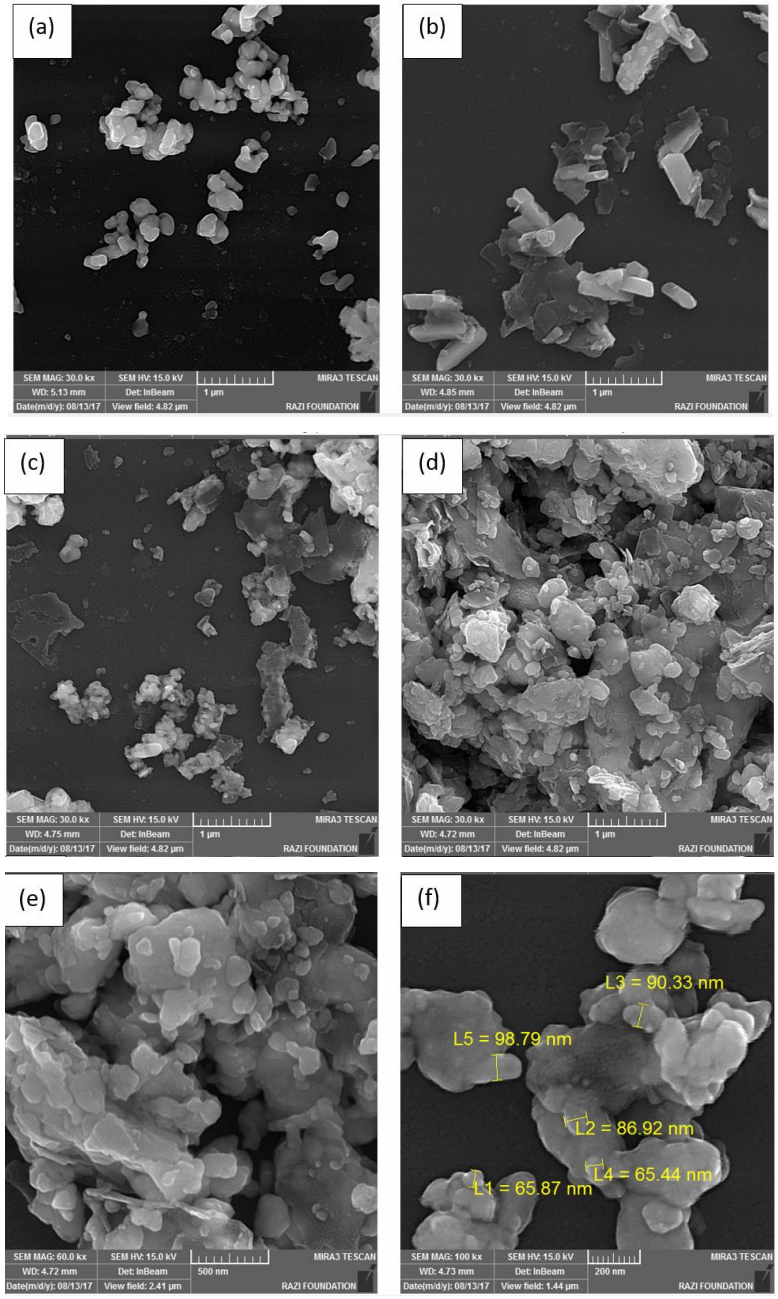

Fig. 6- FESEM images of 10 h milled mixture after reduction at a) 350, b) 550, c) 800 and d, e, f) 1000 °C for 1h.

with high intensities after the heat treatment was due to the stress releasing. Scherrer's formula was used to calculate the crystallite size of molybdenum (42 nm) and copper (37 nm) which were estimated by measuring FWHM of Mo(110) and Cu(111) diffraction peaks.

The effect of mechanical milling followed by the reduction of the microstructures of synthesized powders was also investigated. Fig. 6 shows FESEM images of the 10 h milled mixture after reduction at 350, 550, 800 and 1000 °C. The FESEM images show spherical particles with uniform distributions. In fact due to the high heat treatment temperature to synthesis Mo-Cu alloys, the particle sizes were slightly bigger and the grain growth occurred as compared to the milled sample without a further heat treatment. Fig. 6f shows a high magnified FESEM image of the Mo-Cu alloy. The Mo–Cu alloy powders show spherical shapes with micrometer particle sizes due to agglomeration by the heating at high temperatures.

The sintering temperature has important effects on the electrical conductivity and hardness of sintered Mo-Cu alloys. Table 2 shows that the electrical conductivity and hardness of this alloys were decreased with increasing the sintering

Table 2- Hardness and electrical conductivity of sintered Mo-Cu alloy

Sintering temperature (°C)	Sintering time (min)	Pressure (MPa)	Hardness (HV)	Electrical conductivity (MS/m)
1050	60	700	206.67	10.2
1100	60	700	192.81	6.1
1200	60	700	183.87	7.6

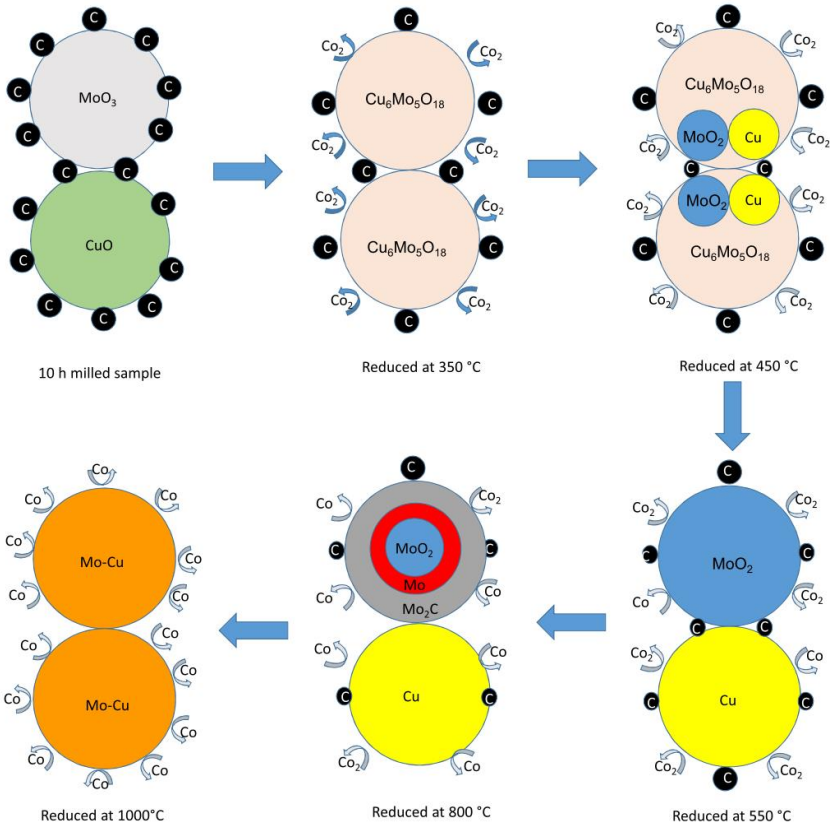

Fig. 7- Schematic mechanism of stepwise carbo-thermic reduction of MoO_3-CuO.

temperature. For the sintered molybdenum-copper alloy, the maximum value of the electrical conductivity and Vickers hardness were measured to be 10.2 MS/m and 206.67 HV, respectively. Wang et. al [13] synthesized Mo–25 wt.%Cu composite powders via the ball milling of the MoO_3 and CuO powders mixture followed by the hydrogen reduction process. The Hardness and thermal conductivity of the Mo–Cu sintered at 1050 °C for 1.5 h were measured to be 214 HV and 22.4 MS/m, respectively. Table 2 also shows that with increasing the temperature of the sintering from 1050 up to 1200 °C, the electrical conductivity and hardness decreased because of the liquid phase sintering and higher values were achieved of those samples produced by solid phase sintering at 1050 °C below the melting point of the copper.

Fig. 7 illustrates a schematic mechanism of the stepwise carbo-thermic reduction of MoO_3-CuO to Mo-Cu and the sequence of processes during reduction is described as follows. Firstly, MoO_3 and CuO react with graphite at 350 °C and $Cu_6Mo_5O_{18}$ phase was formed with oxygen ions diffusion mechanism [28]. This phase formation also was verified by the X-ray diffraction at the early stage of the reduction. At the next step $Cu_6Mo_5O_{18}$ reacts with the graphite at 550 °C to produce MoO_2 and Cu according to the reaction (8).

$$CuMo_5O_{18} + 4C = 5MoO_2 + Cu + 4CO_2 \quad (8)$$

With increasing heat treatment temperature to 800 °C, MoO_2 reacts with the graphite which is in direct contact with MoO_2 on the surface of oxide particles to form Mo because of the high tendency of Mo to react with free carbons in the mixture, after that molybdenum carbide was formed on the surface of MoO_2. In the next step the remaining MoO_2 in the mixture and the synthesized Mo_2C, react with each other to re-synthesize the molybdenum at 1000 °C (reaction 7) [23, 28].

As shown in figure 7 the Mo_2C peaks could be visible with the heating at 800 °C while with increasing the heating temperature to 1000 °C this phase was disappeared. Because of the lower diffusion coefficient of Mo atoms than that of Cu atoms, it could be suggested that Cu was diffused to Mo matrix to synthesize Mo-Cu alloys. In this research Mo-Cu alloys were synthesized because of stacking faults, vacancies and dislocation arrays or energies stored in the nano-crystalline powders. Evolved gases during the carbo-thermal reduction of molybdenum oxides were analyzed in other works and was shown to be a mixture of CO/CO_2 that with increasing the reduction temperature the concentration of CO in the mixture could be increased [29, 30]. Based on the Gibbs free energy changes versus the temperature for the graphite oxidation, CO was more stable than CO_2 at high temperatures when the graphite reacted with the oxygen [25].

4. Conclusions

The results show that with 30 h milling time carbonic-reduction of MoO_3-CuO to Mo-Cu could not be occurred at ambient temperature because of insufficient energy storage. It was shown that Mo-Cu could be synthesized from 10 h mechanically activated MoO_3-CuO mixture with graphite after reduction at 1000 °C for 1 h. Stepwise carbo-thermic reduction and the sequence of processes during reduction was also investigated. The results showed that $Cu_6Mo_5O_{18}$, MoO_2 and Mo_2C phases could be formed during the carbo-thermal reduction process of MoO_3-CuO mixture oxides as intermediate phases. The maximum value of electrical conductivity and the hardness of the Mo–Cu alloy were achieved to be 10.2 MS/m and 209 HV, respectively.

References

1. Sun A, Wang D, Wu Z, Li L, Wang J, Duan B. Microwave-assisted synthesis of Mo–Cu nano-powders at an ultra-low temperature and their sintering properties. Materials Chemistry and Physics. 2014;148(3):494-8.
2. Yao J-T, Li C-J, Li Y, Chen B, Huo H-B. Relationships between the properties and microstructure of Mo–Cu composites prepared by infiltrating copper into flame-sprayed porous Mo skeleton. Materials & Design. 2015;88:774-80.
3. Wang D, Dong X, Zhou P, Sun A, Duan B. The sintering behavior of ultra-fine Mo–Cu composite powders and the sintering properties of the composite compacts. International Journal of Refractory Metals and Hard Materials. 2014;42:240-5.
4. Ke S, Feng K, Zhou H, Shui Y. Sintering process and particles migration mechanism of rapid sintering of W–Cu composites. Materials and Manufacturing Processes. 2017;32(12):1398-402.
5. Shi S, Jin Z, Bao Y, Jiang G. Study of Milling Time and Process Control Agent on W–Mo–Cr Pre-Alloying Powders. Materials and Manufacturing Processes. 2015;31(7):926-32.
6. Johnson JL. Activated liquid phase sintering of W–Cu and Mo–Cu. International Journal of Refractory Metals and Hard Materials. 2015;53:80-6.
7. Aydinyan SV, Kirakosyan HV, Kharatyan SL. Cu–Mo composite powders obtained by combustion–coreduction process. International Journal of Refractory Metals and Hard Materials. 2016;54:455-63.
8. Sun A, Dong X, Wang X, Duan B, Wang D. Synthesis of novel core–shell Cu@Mo nanoparticles with good sinterability. Journal of Alloys and Compounds. 2013;555:6-9.
9. Subject index. Non-equilibrium Processing of Materials: Elsevier; 1999. p. 419-38.
10. Aguilar C, Guzman D, Rojas PA, Ordoñez S, Rios R. Simple thermodynamic model of the extension of solid solution of

Cu–Mo alloys processed by mechanical alloying. Materials Chemistry and Physics. 2011;128(3):539-42.
11. Tan Z, Xue Y-f, Cheng X-w, Zhang L, Chen W-w, Wang L, et al. Effect of element fitting on composition optimization of Al–Cu–Ti amorphous alloy by mechanical alloying. Transactions of Nonferrous Metals Society of China. 2015;25(10):3348-53.
12. Yan J-w, Liu Y, Peng Af, Lu Q-g. Fabrication of nano-crystalline W-Ni-Fe pre-alloyed powders by mechanical alloying technique. Transactions of Nonferrous Metals Society of China. 2009;19:s711-s7.
13. Wang TG, Liang QC, Qin Q. Microstructure and properties of Mo–Cu alloys produced by powder metallurgy. Materials Research Innovations. 2015;19(sup5):S5-1150-S5-2.
14. Martínez VdP, Aguilar C, Marín J, Ordoñez S, Castro F. Mechanical alloying of Cu–Mo powder mixtures and thermodynamic study of solubility. Materials Letters. 2007;61(4-5):929-33.
15. Sabooni S, Mousavi T, Karimzadeh F. Thermodynamic analysis and characterisation of nanostructured Cu(Mo) compounds prepared by mechanical alloying and subsequent sintering. Powder Metallurgy. 2012;55(3):222-7.
16. Xi S, Zuo K, Li X, Ran G, Zhou J. Study on the solid solubility extension of Mo in Cu by mechanical alloying Cu with amorphous Cr(Mo). Acta Materialia. 2008;56(20):6050-60.
17. Aguilar C, Ordóñez S, Marín J, Castro F, Martínez V. Study and methods of analysis of mechanically alloyed Cu–Mo powders. Materials Science and Engineering: A. 2007;464(1-2):288-94.
18. Shkodich NF, Rogachev AS, Mukasyan AS, Moskovskikh DO, Kuskov KV, Schukin AS, et al. Preparation of copper–molybdenum nanocrystalline pseudoalloys using a combination of mechanical activation and spark plasma sintering techniques. Russian Journal of Physical Chemistry B. 2017;11(1):173-9.
19. Sabooni S, Mousavi T, Karimzadeh F. Mechanochemical assisted synthesis of Cu(Mo)/Al2O3 nanocomposite. Journal of Alloys and Compounds. 2010;497(1-2):95-9.
20. Yang H, McCormick PG. Mechanically activated reduction of nickel oxide with graphite. Metallurgical and Materials Transactions B. 1998;29(2):449-55.
21. Zhang DL, Zhang YJ. Chemical reactions between vanadium oxides and carbon during high energy ball milling. Journal of materials science letters. 1998 Jul 1;17(13):1113-5.
22. Sheibani S, Ataie A, Heshmati-Manesh S. Role of process control agent on synthesis and consolidation behavior of nano-crystalline copper produced by mechano-chemical route. Journal of Alloys and Compounds. 2008;465(1-2):78-82.
23. Saghafi M, Ataie A, Heshmati-Manesh S. Effects of mechanical activation of MoO3/C powder mixture in the processing of nano-crystalline molybdenum. International Journal of Refractory Metals and Hard Materials. 2011;29(4):419-23.
24. Cullity BD, Smoluchowski R. Elements of X-Ray Diffraction. Physics Today. 1957;10(3):50-.
25. Gaskell DR. Introduction to the Thermodynamics of Materials, Fifth Edition. CRC Press; 2008.
26. Heidarpour A, Karimzadeh F, Enayati MH. In situ synthesis mechanism of Al2O3–Mo nanocomposite by ball milling process. Journal of Alloys and Compounds. 2009;477(1-2):692-5.
27. Ying DY, Zhang DL. Processing of Cu–Al2O3 metal matrix nanocomposite materials by using high energy ball milling. Materials Science and Engineering: A. 2000;286(1):152-6.
28. Chaudhury S, Mukerjee SK, Vaidya VN, Venugopal V. Kinetics and mechanism of carbothermic reduction of MoO3 to Mo2C. Journal of Alloys and Compounds. 1997;261(1-2):105-13.
29. Gruner W. Determination of oxygen in oxides by carrier gas hot extraction analysis with simultaneous CO x detection. Fresenius' Journal of Analytical Chemistry. 1999;365(7):597-603.
30. Gruner W, Stolle S, Wetzig K. Formation of COx species during the carbothermal reduction of oxides of Zr, Si, Ti, Cr, W, and Mo. International Journal of Refractory Metals and Hard Materials. 2000;18(2-3):137-45.